

Gamma-Ray Bursts as Internal Shocks Caused by DecelerationE. E. Fenimore¹, and E. Ramirez-Ruiz^{1,2}¹MS D436, Los Alamos National Laboratory, Los Alamos, NM 87545²Facultad de Ciencias, Universidad Nacional Autónoma de México, Distrito Federal, México 04510**ABSTRACT**

Gamma-ray bursts (GRBs) have been thought to originate from internal shocks that occur about 10^{15} cm from a central site. The shells responsible for these shocks merge together and undergo an external shock at $\sim 10^{17}$ cm, producing the afterglows. We include deceleration in our model of internal shocks and find that, for values of the Lorentz factor greater than 10^3 , deceleration is an effective catalyst for converting the bulk motion energy into radiation during the GRB phase. Substantial internal energy occurs because other shells run into the back of the first shell which has decelerated and because the first shell must energize the interstellar medium. Whereas internal shocks without deceleration are about 25% efficient, we can convert up to 85% of the bulk motion energy during the GRB phase. We demonstrate that the resulting time history can have three components. The first is due to internal shocks, but not those that involve the first shell. This component produces narrow peaks throughout the time history. The second is due to internal shocks involving the first shell, and it produces progressively wider and wider peaks but they tend to be hidden in a slowly varying background in the event. The third component is from energizing the interstellar medium. It is very smooth and may contribute mostly to a lower energy bandpass than the BATSE experiment. There have been claims of upper limits on the possible Lorentz factor because the deceleration must occur at greater radii than the internal shocks to avoid making progressively wider peaks. We do not find this to be the case, and the Lorentz factor can be much larger.

Subject headings: gamma-rays: bursts

1. INTRODUCTION

Gamma-ray bursts (GRBs) are characterized by chaotic time histories which are often followed by x-ray, optical, and radio afterglows (Metzger et al. 1997, Costa et al. 1997, Frail et al. 1997). The optical afterglows have shown redshifted absorption features which firmly established

a cosmological distance scale for the events. The distance implies that GRBs emit the order of 10^{52} to 10^{54} erg (assuming isotropic emission). GRBs are also often characterized by emission up to 100 MeV with occasional reports of emission up to 10 GeV (Hurley et al. 1994). Given the photon density implied by the cosmological distances, photons above ~ 1 MeV would be destroyed by photon-photon attenuation if the emission is isotropic in our rest frame. Large relativistic bulk motion (Lorentz factors of $\gtrsim 100$) allows for a much larger emitting surface combined with relativistic beaming that reduces the photon-photon attenuation (Fenimore, Epstein, & Ho 1993).

The high Lorentz factor plays a crucial role in virtually all models of GRBs. Originally, the prime suspect for the source of 10^{52} erg was a neutron star-neutron star merger (Paczynski 1986). However, such mergers were thought to occur on timescales (a few millisecond) much shorter than GRB timescales (up to 10^3 sec). Mészáros & Rees (1993) suggested that a relativistic shell would be formed by the initial release of energy. The shell could emit for a long time (10^7 sec). If the shell is mostly moving directly at the observer, the shell stays close to the photons it emits such that they all arrive at a detector over a short period of time. If the shell moves with velocity v , then photons emitted over a duration Δt arrive at the detector compressed into a duration of only $(c - v)\Delta t/c \approx \Delta t/(2\Gamma^2)$ where Γ is the bulk Lorentz factor $= (1 - \beta^2)^{-1/2}$ and $\beta = v/c$. The shell would emit due to the formation of an “external” shock when the shell decelerates by sweeping up the interstellar medium (ISM). In this explanation, density variations in the ISM cause the observed time structure. The deceleration is expected to occur at

$$R_{\text{dec}} = 5(\rho E_0)^{1/3} \Gamma_0^{-2/3} \text{cm} \quad (1)$$

where ρ is the ambient density (in cm^{-3}), E_0 is total energy (in erg) generated by the central site, and Γ_0 is the initial Lorentz factor (Rees & Mészáros 1994). For typical values such as $\rho = 1 \text{ cm}^{-3}$, $E_0 = 10^{53}$ erg, and $\Gamma_0 = 100$, the deceleration occurs at about 10^{17} cm. The initial Lorentz factor is set by the baryon loading, that is

$$E_0 = \Gamma_0 m_0 c^2 \quad (2)$$

where m_0 is the mass of the shell, presumably carried by the baryons.

An alternative explanation is that the central site produced a series of shells. Collisions between shells produce the gamma rays through internal shocks (Rees & Mészáros 1994). The faster shells catch up with the slower shells. The collision radius is roughly

$$R_{\text{col}} = c\Gamma^2\Delta T \quad (3)$$

where ΔT is a typical time of variation in a GRB (Rees & Mészáros 1994). For typical values such as $\Delta T = 0.1$ to 1.0 s, R_{col} is about 10^{15} cm. The observed duration of the GRB is set by the duration of the activity at the central site.

There are a series of arguments that indicate that the gamma-ray phase is not caused by external shocks. These arguments are all related to the fact that the size of the shell at the

deceleration radius is much larger than a causally connected region on the shell. For example, precursors and gaps require large causally disconnected regions to coordinate their activity (Fenimore, Madras, & Nayakshin 1996). The observed variability implies that only a small fraction of the shell emits (Fenimore et al. 1996, Sari & Piran 1997), and the average profile of many GRBs is inconsistent with that expected from a shell (Fenimore 1999). Finally, the constancy of the pulse width throughout the bursts indicates that we are not seeing a range of angles on a shell and that the shell is not decelerating (Ramirez-Ruiz & Fenimore 1999a). A single decelerating shell would produce pulses that get progressively wider.

However, external shocks have been very successful in explaining the x-ray, optical, and radio afterglows (see review by, e.g., Piran (1999)). These afterglows usually show power law decays and spectral variability expected from a decelerating shell. Thus, a general picture has formed where the central site produces multiple shells for tens of seconds. These shells collide, producing the gamma-ray phase by internal shocks and then merge into a single shell which interacts with the ISM to produce the afterglows (Sari & Piran 1997). One-dimensional hydrodynamical calculations have reproduced many of the features of the spectral evolution (Panaitescu & Mészáros, 1998). There have been several detailed calculations of what is expected from the internal shocks. Mochkovitch, Maitia, & Marques, (1995), Kobayashi, Piran, & Sari (1997), and Daigne & Mochkovitch (1998) used Monte Carlo calculations of internal shocks where the Γ , mass, time, and thickness of multiple shells are picked randomly to demonstrate that internal shocks can produce the variability seen in GRBs. By following their trajectories, it is determined when they collide. The duration of the resulting simulated GRBs is effectively the duration of the activity at the central site. The rise of each pulse depends on the time for a reverse shock to cross the shell and the fall depends on the curvature of the shell at the radius of interaction (Kobayashi, Piran, & Sari (1997)). The radius of interaction depends on the Lorentz factors and the amount of time between the production of the shells at the central site. Indeed, the resulting time histories bear some similarities to the observed bursts.

The strong optical emission discovery by the Robotic Optical Transient Search Experiment, ROTSE, (Akerlof et al. 1999) as served as an excellent test case for the external shock model. Sari & Piran (1999) and Mészáros & Rees (1999) fit forward and reverse external shocks and had excellent agreement with the time of the optical peak, the rise and fall times, the overall magnitude, and the break in the decay phase.

2. The Role of Γ

The Lorentz factor is not well determined observationally. The lack of apparent photon-photon attenuation up to ~ 100 MeV implies only a *lower* limit of ~ 100 (Fenimore, Epstein, & Ho 1993). The Γ determined by Sari & Piran (1999) for GRB990123 depended on some parameters adopted from Wijers & Galama (1999) for GRB970508, but gave a similar low value of $\Gamma = 200$. However, there have been recent reports of possible TeV emission from GRBs (Lemon et al., 1999) implying

that Γ may be much larger. Also, if Γ is small, the efficiency of internal shocks is small, the order of 10%.

The first shell starts to decelerate when it has swept up $\sim \Gamma^{-1}$ of its initial mass. Thus, larger Γ means the deceleration will occur at a smaller radius. But, a larger Γ means that the multiple shells will collide at a larger radius. Combining equations (1) and (3), internal shocks will occur at about the same radii as the deceleration if $\Gamma \gtrsim 10^{-10}(\rho E_0)^{1/4}$. From the few observed redshifts, we know that GRBs have a rather large range of fluences, with typical values between 10^{52} and 10^{54} erg for isotropic emission. We have little direct knowledge of the ambient density in the vicinity of a GRB, but it is reasonable to assume values of ρ between 0.1 and 10.0, so ρE_0 varies from 10^{51} to 10^{55} erg cm $^{-3}$. For values of Γ of ~ 500 to 3000, the internal shocks will occur about the same place as the deceleration.

Once the first shell decelerates (making an external shock), the rest of the shells will rapidly catch up to it resulting in rather efficient internal shocks. In previous models (e.g., Kobayashi et al. 1997), Γ was about 10^2 to 10^4 but deceleration was not included. It was assumed that the internal shocks would form at small radii and later the merged shell would suffer deceleration and an external shock. Perhaps a few straggler shells would catch up to the first shell after it decelerated and rejuvenate it during the afterglow phase (Panaitescu, Mészáros, & Rees, 1998), but most of the gamma-rays were assumed to form at small radii relative to the external shock.

We propose that the typical Lorentz factor is large enough such that the first shell decelerates before all of the multiple shells have a chance to collide. The deceleration is very rapid once it starts, effectively equivalent to slamming on the breaks. The rest of the shells catch up and collide with it. Since the efficiency of converting bulk motion to radiation in an internal shock depends on the difference of the colliding Γ 's, the fact that the first shell is decelerating implies that the efficiency will be higher than in previous models. Thus, the collisions are internal shocks but the place and efficiency of the many of collision are caused by deceleration.

3. Ingredients for a Model

In the internal shock model, multiple shells are generated by an unspecified process at a central site. The parameters of our model will be similar to those of Mochkovitch, Maitia, & Marques, (1995), Kobayashi et al. (1997) and Daigne & Mochkovitch (1998), including the time the i -th shell was generated (t_{0i}), the initial width of the shell (l_i), the minimum and maximum initial Lorentz factor ($\Gamma_{\min}, \Gamma_{\max}$), and the initial energy (E_i). Kobayashi et al. (1997) allowed for selecting the initial mass, energy, or density. However, all three gave similar results and we will restrict ourselves to selecting the energy. The initial m_i is then found from equation (2). Since Kobayashi et al. (1997) presented unitless intensities, it was unnecessary for them to specify E_i . The bulk energy is necessary to set the deceleration. The peak energy can be estimated from bursts with observed redshifts. GRB970508 had a peak luminosity, L , of $\sim 3 \times 10^{51}$ erg s $^{-1}$. Other

GRBs have shown extreme redshifts (e.g., Kulkarni et al. 1999), implying $L \sim 2 \times 10^{53}$ erg s⁻¹. We will uniformly select E_i between E_{\min} ($=10^{49}$ erg s⁻¹) and E_{\max} , and vary E_{\max} from 10^{51} to $10^{53.5}$ erg.

We randomly select $t_{0i+1} - t_{0i}$ from a Poisson distribution based on the rate of peak occurrence. Thus, we specific the duration of the activity at the central site (T_{dur}) and the expected number of peaks (N) such that the actual number of peaks is random. Since they were presenting results in unitless time, Kobayashi et al. (1997) set the burst duration, shell separation, and the number of peaks to be constants. These differences are not important when there is no deceleration. We will use parameters that are roughly equivalent to Kobayashi et al. (1997), that is, $N = 85$, $T_{\text{dur}} = 60$ s, and $l_i = 0.2$ s. Burst often have gaps which implies that the activity at the central site can turn off for a while. To demonstrate the effects of turning off the central site, we impose a gap in the activity between $T = 20$ and $T = 33$ s.

Until they collide with the first shell or each other, the motion of the every shell except the first is constant, $R_i(t) = c\beta_i(t - t_{0i})$. If Γ_i is greater than Γ_j , the two shells will collide at time t_{ij} when $R_i(t_{ij}) = R_j(t_{ij})$, which we call the collision radius ($=R_c$), and it occurs at

$$t_{ij} = 2 \frac{\Gamma_i^2 \Gamma_j^2}{\Gamma_i^2 - \Gamma_j^2} \Delta t_{0ij} \quad (4)$$

where $\Delta t_{0ij} = t_{0i} - t_{0j}$. The resulting pulse arrives at a detector at the relative time of arrive

$$T_{\text{toa}} = t_{ij} - R_c/c = t_{0i} + \frac{\Gamma_j^2}{\Gamma_i^2 - \Gamma_j^2} \Delta t_{0ij} \quad . \quad (5)$$

Thus, the relative time of arrival at a detector will have a close one-to-one relationship with the time the shell was created (i.e., t_{0i}).

In order to conserve both momentum and energy when shells collide, some of the bulk energy must be converted to internal energy which will be radiated away. If E_{rad} is the generated internal energy, conservation of energy dictates that

$$m_i \Gamma_i + m_j \Gamma_j = [m_{ij} + \frac{E_{\text{rad}}}{c^2}] \Gamma_{ij} \quad (6)$$

where Γ_{ij} is the Lorentz factor of the resulting shell and the resulting mass is $m_{ij} = m_i + m_j$. Conservation of momentum gives:

$$m_i \beta_i \Gamma_i + m_j \beta_j \Gamma_j = [m_{ij} + \frac{E_{\text{rad}}}{c^2}] \beta_{ij} \Gamma_{ij} \quad (7)$$

where, as usual, the Γ terms are related to the β terms as $\Gamma = (1 - \beta^2)^{-1/2}$. The post collision β is

$$\beta_{ij} = \frac{m_i \beta_i \Gamma_i + m_j \beta_j \Gamma_j}{m_i \Gamma_i + m_j \Gamma_j} \quad (8)$$

which has the approximate solution (Kobayashi et al. 1997)

$$\Gamma_{ij}^2 = \Gamma_i \Gamma_j \frac{m_i \Gamma_i + m_j \Gamma_j}{m_i \Gamma_j + m_j \Gamma_i} . \quad (9)$$

The first shell is decelerated by the ISM. We use equations 7 and 6 with $\Gamma_j = 1$ and m_j equal to the mass swept up during the time step to determine the velocity of the first shell as a function of time.

The colliding shells make a peak in the gamma-ray time history at relative time $t_{ij} - R_c/c$. When two shells collide, forward and reverse shocks traverse the shells. If the internal energy is promptly converted into radiation, the merged shell emits for about the time that it takes for the reverse shock to cross the shell (see Kobayashi et al. 1997). The Γ factors for the forward and reverse shocks are found from Sari & Piran (1995)

$$\Gamma_{fs} = \Gamma_{ij} \left[\frac{1 + 2\Gamma_{ij}/\Gamma_i}{2 + \Gamma_{ij}/\Gamma_i} \right]^{1/2} \quad (10)$$

and

$$\Gamma_{rs} = \Gamma_{ij} \left[\frac{1 + 2\Gamma_{ij}/\Gamma_j}{2 + \Gamma_{ij}/\Gamma_j} \right]^{1/2} . \quad (11)$$

4. Pulse Shape

A shell that coasts without emitting photons and then emits for a short period of time produces a pulse with a rise time related to the time the shell emits and a decay dominated by curvature effects (Fenimore et al. (1996)). In the internal shock model, the shell emits for the time it takes the reverse shock to cross the shell that is catching up, that is (Kobayashi et al. 1997),

$$\Delta t_{\text{cross}} = l_j / (\beta_j - \beta_{rs}) . \quad (12)$$

The time of arrival at a detector (relative to the start of the pulse) of photons generated at angle θ from the line of sight is

$$T(\theta) = R_c(1 - \cos \theta)/c \quad (13)$$

(Note in our previous papers, it was more convenient to measure time from when the shell left the central site; this is not used here because the shell does not move at a constant speed.) At angle θ , the Doppler factor, Λ , is $\Gamma_{ij}(1 - \beta_{ij} \cos \theta)$. At time T in the pulse, the Λ factor is

$$\Lambda(T) = \frac{R_c + 2\Gamma_{ij}^2 c T}{2\Gamma_{ij} R_c} \quad (14)$$

To calculate the observed pulse shape, one needs to combine the Doppler beaming with the volume of material that can contribute at time T . Following the method in Summer & Fenimore (1998),

the resulting pulse shape is

$$\begin{aligned}
 V(T) &= 0 && \text{if } T < 0 \\
 &= \psi \frac{(R_c + 2\Gamma_{ij}^2 cT)^{\alpha+3} - R_c^{\alpha+3}}{(R_c + 2\Gamma_{ij}^2 cT)^{\alpha+1}} && \text{if } 0 < 2\Gamma_{ij}^2 T < \Delta t_{\text{cross}} \\
 &= \psi \frac{(R_c + \Delta t_{\text{cross}})^{\alpha+3} - R_c^{\alpha+3}}{(R_c + 2\Gamma_{ij}^2 cT)^{\alpha+1}} && \text{if } 2\Gamma_{ij}^2 T > \Delta t_{\text{cross}}
 \end{aligned} \tag{15}$$

where ψ is a constant and T is measured from the start of the pulse.

The cooling is very rapid so the internal energy generated by the collision, E_{rad} , is immediately turned into photons. An observer, using a detector such as BATSE, sees the fraction that is in the BATSE bandpass of 50 to 300 KeV, f_{BATSE} . Since we do not understand exactly how the internal energy is distributed, we cannot predict f_{BATSE} . However, GRB often have a ‘‘Band’’ spectral shape with $\alpha = -1$, $\beta = -2.5$, and $E_{\text{peak}} = 250$ KeV (Band et al. 1993). If that shape is valid over the entire range of emission, f_{BATSE} is ~ 0.37 . We generate simulated time histories as the sum of pulses with the shape from equation (15) and integrated fluence of $f_{\text{BATSE}} E_{\text{rad}}$. We generate the time history with 0.064 s samples (to mimic BATSE) and then find the peak emitted luminosity in 0.256 s ($= L_{256}$). Ignoring cosmological redshift effects, the BATSE catalog value of P_{256} should be related to L_{256} .

5. A Typical Simulation

To summarize our model, we have eight parameters: the duration of the activity (T_{dur}), the rate of explosions at the central site (N/T_{dur}), the range of Lorentz factors ($\Gamma_{\text{min}}, \Gamma_{\text{max}}$), the range of energy release at the central site ($E_{\text{min}}, E_{\text{max}}$), the ISM density (ρ), and the range of initial thicknesses (0 to l). To be comparable to Kobayashi et al. (1997), we will set $N = 85$, $T_{\text{dur}} = 60$ s, and $l = 0.2$ s. Kobayashi et al. (1997) parameterized much of their results based on $\Gamma_{\text{max}}/\Gamma_{\text{min}}$ since the overall efficiency of the conversion of bulk energy to radiation was primarily dependent on that parameter. With deceleration, we have found that the efficiency depends mostly on Γ_{max} , so we have set Γ_{min} to the minimum required for the high energy emission (100), and varied Γ_{max} from $10^{2.5}$ to $10^{4.5}$. Kobayashi et al. (1997) had no analog to $E_{\text{min}}, E_{\text{max}}$, and ρ . Since we selected E uniformly between E_{min} and E_{max} , E_{min} is not important as long as it is much less than E_{max} . We set E_{min} to 10^{49} erg. For ρ we have used 1 cm^{-3} .

Figure 1 is a typical simulation $E_{\text{max}} = 3.6 \times 10^{53}$ erg, $\Gamma_{\text{max}} = 3.2 \times 10^4$. In Figure 1a, ρ is zero, so there is no deceleration. About 1.5×10^{55} erg (assuming isotropy) were released at the central site in 81 shells. The burst duration at the observer is approximately the duration of the activity at the central site. About 25% of the bulk energy was received by the observer in the period T_{dur} . Figure 1b is the same simulation (i.e., same set of random numbers), but includes deceleration of the first shell in an ISM with $\rho = 1 \text{ cm}^{-3}$. Both simulations appear similar because

both reflect the activity of the central engine (see eq. [5]). The dotted line is the contribution to the time history from collisions with the first shell. It tends to add a DC level with a few wide peaks but it raises the fraction of the bulk energy converted to radiation to 45%. Some of the radiation will arrive after T_{dur} because curvature will delay it.

Figure 2a gives the Lorentz factor for the first shell in Figure 1b. Given the high value of Γ_{max} , it quickly decelerates but other shells collide with it, giving it a boost and maintaining a large Γ for most of the burst. The deceleration occurs because the first shell collides with the ISM. The resulting internal energy must also radiate away. In Figure 2b we show the contribution to the time history of Figure 1 from the internal energy from the deceleration if it radiates in the BATSE bandpass. It tends to be smooth and would fill in gaps if it had a f_{BATSE} similar to that from the internal shocks. We define $E_{\text{dec,dur}}$ to be the internal energy generated by the collision of the first shell with the ISM that would arrive at the detector with $T_{\text{toa}} < T_{\text{dur}}$. For the case in Figure 1, $E_{\text{dec,dur}}$ is 38% of the bulk motion energy.

6. Efficiency of Converting Bulk Energy

The efficiency of the conversion is an important constraint. Although the time histories imply that GRBs are central engines with internal shocks, internal shocks usually do not convert most of the bulk motion into energy (e.g., $\lesssim 25\%$, Kobayashi et al. 1997). Observationally, the afterglows only account for a small percentage of the energy so it is not clear where most of the energy goes. The efficiency for an individual collision can be found from the initial and final bulk energies:

$$\epsilon_{ij} = 1 - \frac{m_{ij}\Gamma_{ij}}{m_i\Gamma_i + m_j\Gamma_j} \quad (16)$$

If there is no deceleration, the shells will collide until the remaining shells are ordered with decreasing value of the Lorentz factors. Let n be the number of remaining shells. The overall efficiency depends on how much energy remains in un-collided shells:

$$\epsilon = 1 - \frac{\sum_{ij=0}^{ij=n} m_{ij}\Gamma_{ij}}{\sum_{i=0}^{i=N} m_i\Gamma_{0i}} \quad (17)$$

When deceleration occurs, n is 1, another reason why our model will give higher efficiency than previous models.

To study the effects of deceleration we have generated sets of 128 bursts, under a variety of conditions. Figure 3 shows the average efficiency as a function of Γ_{max} . The curves labeled “No Deceleration” is effectively the same result as Kobayashi et al. (1997). The curves labeled “Deceleration, IS” includes an ISM with $\rho = 1 \text{ cm}^{-3}$. We ran models for a range of E_{max} (maximum energy per shell) and interpolated the results to find the efficiency at three values of the peak L_{256} in the time histories: 3×10^{50} , 3×10^{51} , and $3 \times 10^{52} \text{ erg s}^{-1}$ (the solid, dotted, and dashed lines, respectively). Figure 4 shows the corresponding average radii for the internal shocks

that produces pulses that arrive with $T_{\text{toa}} < T_{\text{dur}}$, that is, during the GRB phase. (Including all internal shocks would produce a misleading result when there is little deceleration because a few stragglers would finally collide at radii orders of magnitude larger.) The curves labeled “ES” are the average radii at which the Lorentz factor of the first shell is reduced by half. Once the first shell starts to decelerate, a fair number of the shells collide with it, raising the average amount of the bulk energy which is released in internal shocks. These collisions are more efficient since there is a greater disparity between the Γ factors. For large values of Γ_{max} , the efficiency rises to 40%.

The curves labeled “Deceleration, IS” in Figure 3 are based on the ratio of the internal energy generated by collisions between shells (including the first shell) to the total generated bulk motion energy. It does not include the bulk motion energy lost to energizing the ISM. Eventually, all of the bulk motion energy is lost to the ISM. In previous models it was assumed that this was far from where the internal shocks occur. In the curves labeled “Deceleration, IS+ES”, we include $E_{\text{dec,rad}}$ in the efficiency, that is, the internal energy from collision with the ISM whose photons would start to arrive during the burst. For large values of Γ_{max} , nearly 85% of the bulk motion energy is lost during the GRB phase.

7. DISCUSSION

Internal shocks are capable of producing the variability that is the signature of GRBs (Kobayashi et al. 1997). However, it has been believed that internal shocks are inefficient, converting only $\lesssim 25\%$ of the bulk motion energy into radiation. Since the afterglows only account for a few percent of the radiated energy, it has been unclear where most of the energy goes.

In this paper, for the first time, deceleration of the first shell is included in an internal shock model. For $\Gamma_{\text{max}} \gtrsim 10^3$, there are two ways that deceleration is an important catalyst for converting bulk motion into radiation. First, the deceleration occurs because the bulk motion must energize the ISM that it runs into. Much of the energy to energize the ISM goes into internal energy. This is rather effective because the bulk motion energy of the first shell is $\Gamma_i M_i c^2$ where the mass grows as other shells run into the first shell. If deceleration causes the Γ of the first shell to drop by 50%, nearly 50% of the bulk motion energy will be used. Second, the rapid deceleration causes shells to plow into the back of the first shell. The efficiency for converting bulk motion (for equal mass shells) scales as $1 - (\Gamma_j/\Gamma_i)^{1/2}$ if Γ_i is much larger than Γ_j , as is the case when the j -th shell is decelerating. These two effects combine to release up to 85% of the bulk motion energy while T_{toa} is less than T_{dur} , that is, during the GRB phase. Although the bulk motion might be effectively converted to internal energy, the resulting electron distribution is difficult to predict, so we do not know how much of it will occur in the BATSE bandpass (i.e., f_{BATSE} is uncertain).

Thus, one can identify three types of contributions to the time history, each with a different character. The internal shocks that do not involve the first shell, internal shocks involving the first shell, and the external shock produced as the first shell decelerates.

The internal shocks that do not involve the first shell are characterized by narrow pulses, and have nearly constant width throughout the time history (see, for example, Fig. 1a). The T_{toa} for these pulses is dominated by the time the shells were produced at the central site (following eq.[5]). They occur at a similar radius from the central site. If Γ_i is selected randomly between a small Γ_{min} and Γ_{max} , many pulses form with a similar Lorentz factor: $\Gamma_{ij} \sim (\Gamma_i \Gamma_j)^{1/2} \sim \Gamma_{\text{max}}/2$. The pulse shape depends mostly on R_c and Γ_{ij} (eq. [15]), so they are quite similar.

The internal shocks involving the first shell occur at ever increasing radii with a generally decreasing Lorentz factor. Thus, equation (15) produces peaks that are wider and wider (see the dotted curve in Fig. 1b). In our previous papers, we argued that the time history could not arise from a *single* shell because the pulses did not get wider and wider. This argument is still valid and this paper shows how *multiple* shells can produce narrow peaks throughout the event in the presence of wider and wider pulses from a single shell. Indeed, a recent analysis of 387 pulses in 28 BATSE GRBs shows that the most intense pulses in a burst have nearly identical widths throughout the burst, but the weak pulses show a trend to become wider as the burst progresses (Ramirez-Ruiz & Fenimore 1999b). This is precisely what is seen in simulations when deceleration is included.

There have been claims of upper limits on the possible Lorentz factor because the deceleration must occur at greater radii than the internal shocks (Lazzati, Ghisellini, & Celotti 1999) to avoid making progressively wider peaks. We do not find this to be the case, and the Lorentz factor can be much larger, allowing more of the bulk motion energy to be released during the GRB phase.

The third type of contribution arises from the external shock as the first shell energizes the ISM. This is a smooth component with some variation as the Lorentz factor increases due to collisions with faster shells and decreases due to deceleration (see Fig. 2b). Previous external shock models (e.g., Dermer & Mitman 1999) have assumed the shock interacts with ISM clouds that are much smaller than the size of the shell. This was necessary to produce the temporal variability. We do not assume any structure in the ISM so the contribution from this component is quite smooth.

Figure 5 shows BATSE time histories that have the characteristics of our simulations. Figure 5a is BATSE burst 2831. It has many narrow peaks throughout the time history but also gaps that go back to background. The presence of gaps implies little deceleration of the first shell because the gaps are not filled in. The gaps would occur because the central site turns on and off. We note that this burst is the record holder for the highest energy photons, 18 GeV (Hurley et al. 1994).

Figure 5b is BATSE burst 2329, and initially, it shows narrow peaks, but then broader peaks, on top of a slower varying level. The structure on the rise in burst 2329 is statistically significant. The slower varying function and widening pulses implies substantial deceleration of the first shell. In other bursts (e.g., BATSE burst 130), there are gaps where the last pulse before the gap has a slow decay, similar to that seen in Figure 1b. However, these gaps can go all the way down to the background. Such bursts seem to show the signature of internal shocks on a decelerating first

shell but not the contribution from the energization of the ISM. Since we do not understand the mechanism by which the internal energy is distributed, the f_{BATSE} values associated with each component might be different and the emission might appear in different bandpasses. Perhaps the f_{BATSE} for energizing the ISM is small and its internal energy is radiated at lower energy such as the x-ray excesses reported by Preece et al. (1995).

Apparently, some bursts involve deceleration and some do not. The Lorentz factor required to have deceleration depends very weakly on ρ and E_0 (i.e., $(\rho E_0)^{1/4}$). Thus it seems more likely that intrinsic variations in Γ_{max} might be the reason why some bursts show more deceleration than others.

If the prompt emission is caused by the first shell, as suggested by the analysis of GRB990123 (Sari & Piran 1997), we would expect events with a slowly varying component to be more likely to show prompt, bright optical emission or early afterglows.

In summary, it is possible to convert a large fraction ($\sim 85\%$) of the bulk motion energy into radiation during the gamma-ray burst phase with internal shocks if deceleration of the first shell is accounted for and the Lorentz factor is $\gtrsim 10^3$.

acknowledgment: The authors gratefully acknowledge useful conversations with Re'em Sari.

REFERENCES

- Akerlof, C. W., et al. 1999, *Nature* 398, 400
- Band, D., et al., 1993, *ApJ*, 413, 281
- Costa, E., et al., 1997, *Nature*, 387, 783
- Daigne, F., & Mochkovitch, R., 1998, *MNRAS*, 296, 275
- Dermer, C. D., & Mitman, K. E., 1999, *ApJ*, submitted, astro-ph/9809411
- Fenimore, E. E., 1999, *ApJ*, 518, 375
- Fenimore, E. E., Epstein, R. I., & Ho, C., 1993, *A&A Supp.* 97, 59
- Fenimore, E. E., Madras, C. D., & Nayakshin, S., 1996, *ApJ* 473, 998, astro-ph/9607163
- Frail, D., Kulkarni, S. R., Nicastro, L., Feroci, M., & Taylor, G. B., 1997, *Nature*, 389, 261
- Hurley, K., et al., 1994, *Nature* 372, 652
- Kobayashi, S., Piran, T., & Sari, R., 1997, *ApJ* 490, 92
- Kulkarni, S., et al. 1999, *Nature* 398, 389
- Lazzati, D., Ghisellini, G, & Celotti, A., 1999, submitted to *MNRAS*, astro-ph/9907070
- Leonor, I., et al., 1999, *Proc. of 26th ICRC (Salt Lake City)*, in press
- Mészáros, P., & Rees, M. J., 1993, *ApJ*, 405, 278
- Mészáros, P., & Rees, M. J., 1999, submitted to *ApJL*, astro-ph/9902367
- Metzger, M. R., et al. 1997, *Nature*, 387, 878
- Mochkovitch, R., Maitia, V., & Marques, R. 1995, in *Towards the Source of Gamma-ray Bursts*,
Proceeding of the 29th ESLAB Symposium, eds, Bennett, K., & Winkler, C., pg 531
- Paczynski, B., 1986, *ApJL* 308, L43
- Panaitescu, A., & Mészáros, P., 1998, *ApJ* 492, 683
- Panaitescu, A., Mészáros, P., & Rees, 1998, *ApJ* 503, 314
- Piran, T., 199, *Physics Reports*, 1319, 575
- Preece, R., et al., 1995, *Astro. & Space Sci.*, 231, 207
- Ramirez-Ruiz, E., & Fenimore, E. E., 1999a, *A&A Supplement*, *Proc. Of the Rome Conf. Gamma-Ray Bursts in the Afterglow Era*, in press, astro-ph/9812426

Ramirez-Ruiz, E., & Fenimore, E. E., 1999b, to be submitted to ApJ

Rees, M. J., & Mészáros, P., 1992, MNRAS 258, P41

Rees, M. J., & Mészáros, P., 1994, ApJ, 430, L93

Sari, R., & Piran, T., ApJ, 455, L143

Sari, R., & Piran, T., 1997, ApJ, 485, 270

Sari, R., & Piran, T., 1999, ApJL,

Summer, M. C., & Fenimore, E. E., Gamma-Ray Bursts: 4-th Huntsville Symposium, eds. Meegan, Preece, & Koshut, (AIP Proc 428) pg 765, astro-ph/9712302

Wijers, R. A. M. J., & Galama, T. J., 1999, ApJ, submitted, astro-ph/98053451

Fig. 1.— Simulated GRB time histories. (a) A simulated GRB time history from internal shocks with no deceleration. The Lorentz factors were chosen uniformly between 10^2 and $10^{4.5}$ and the peak luminosity (found over 256 ms) is $L_{256} = 2 \times 10^{53}$ erg s $^{-1}$. Shells were randomly created at the central site for 60 sec except for a 13 s period, thus producing a gap in the simulated GRB time history. About 25% of the bulk motion was converted into radiation by the internal shocks. (b) Simulated GRB time history from internal shocks including deceleration of the first shell due to an ISM with 1 particle cm $^{-3}$. The same random numbers as in (a) were used. The lower curve is the contribution to the time history from collisions with the decelerating shell. Note that there are still many narrow spikes throughout the event. There is a slower decay during the gap. About 45% of the bulk motion was converted into radiation by the internal shocks.

Fig. 2.— (a) The Lorentz factor of the decelerating shell in Figure 1 as a function of when photons would arrive from it. The Lorentz factor is fairly constant for much of the burst because shells continue to collide with it. (b) The expected time history from the bulk motion energy that is converted into internal energy by the collision of the first shell with the ISM. It is smooth and would fill in gaps in the time history.

Fig. 3.— The efficiency of converting bulk motion into internal energy as a function of the maximum Lorentz factor. If there is no deceleration (ISM density = 0), the maximum efficiency is about 25%. If deceleration is included, the internal shocks convert up to 45% of the bulk motion to internal energy. The deceleration is caused by an external shock that sweeps up and energizes the ISM. The curve labeled “Deceleration, IS+ES” gives the fraction of the total original bulk energy that is lost from the shells (some into internal shocks, some to energized the ISM). Up to 85% of the original energy is used during the GRB phase if the Lorentz factor is as large as 3×10^4 .

Fig. 4.— The radii for deceleration and internal shocks. The solid, dotted, and dashed lines are for increasing values of L_{256} . The curves labeled “ES” are the average radii when the Lorentz factor of the first shell first drops to half its original value. The curves labeled “IS” are the average radii for internal shocks that produce peaks during the GRB phase. For Lorentz factors greater than ~ 3000 , many of the internal shocks are caused by shells running into the back of the first shell which is undergoing deceleration.

Fig. 5.— The time history of long BATSE GRBs. (a)BATSE burst 2831 which is consistent with internal shocks with very little deceleration. Note that the gaps are near background and the decay into the gaps is sharp. (b)BATSE burst 2329 which is consistent with substantial deceleration. Note that the peaks tend to get progressively wider and there is an underlying smooth component.

Figure 1

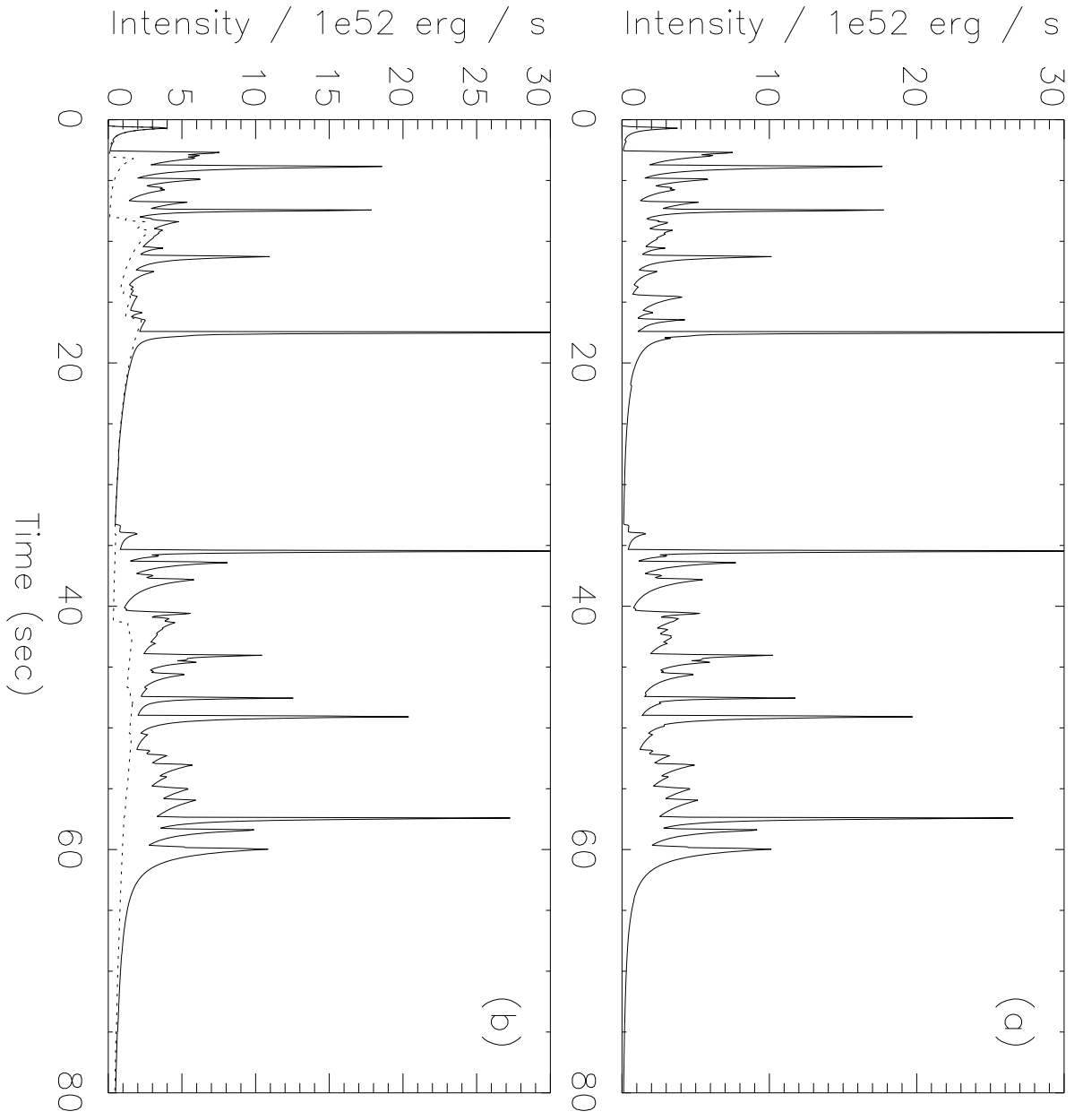


Figure 2

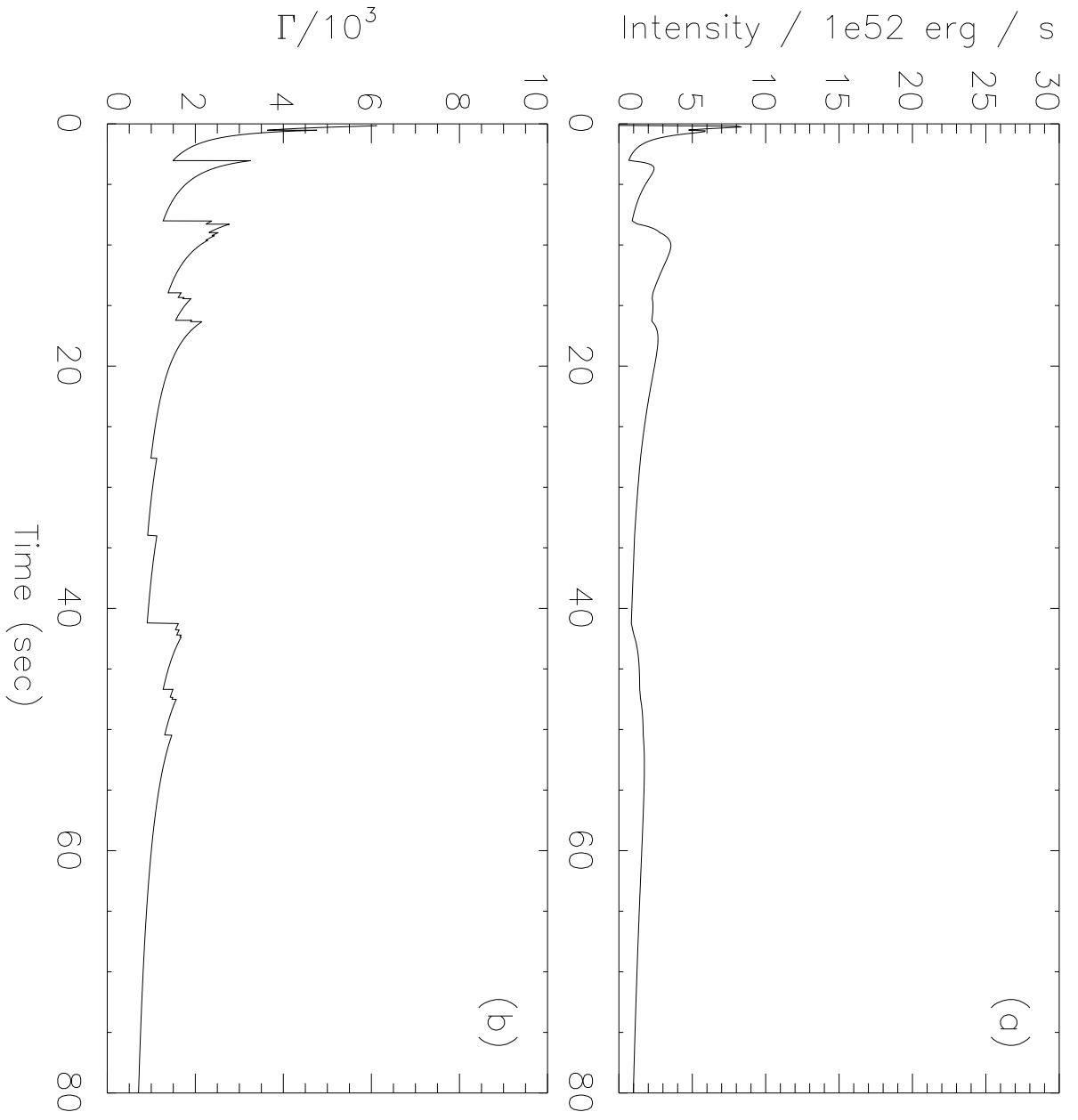


Figure 3

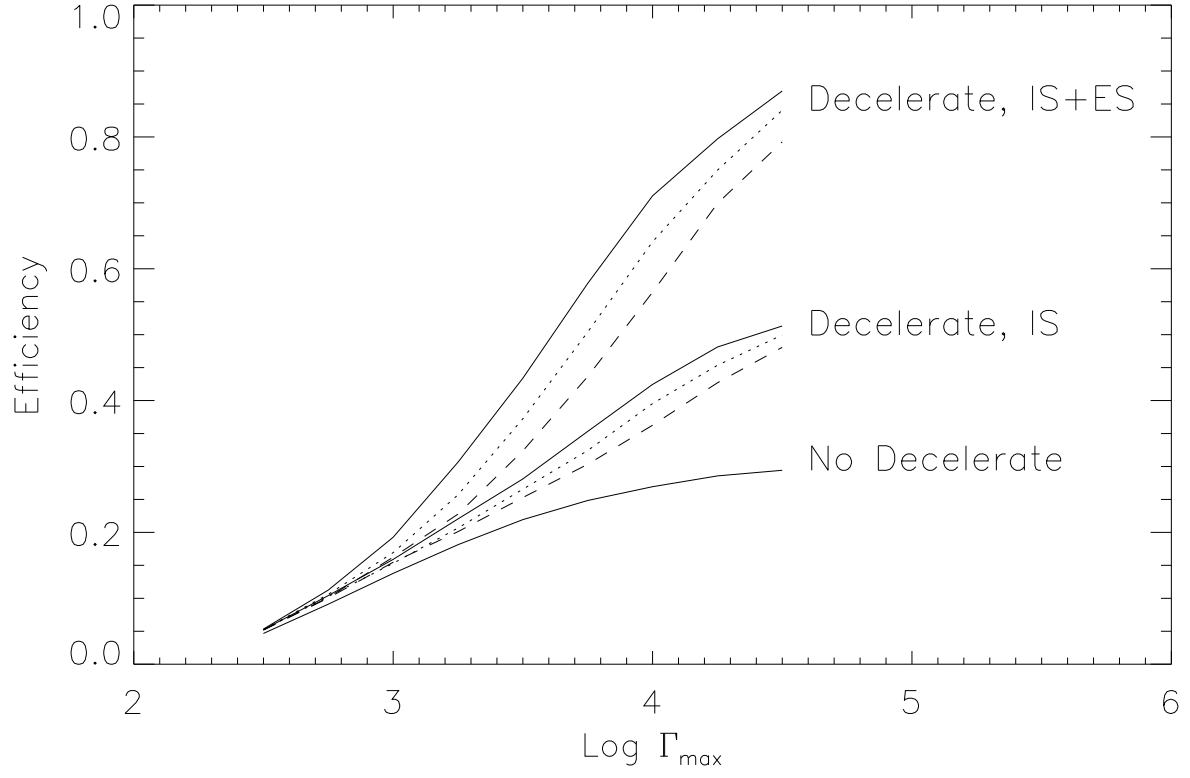


Figure 4

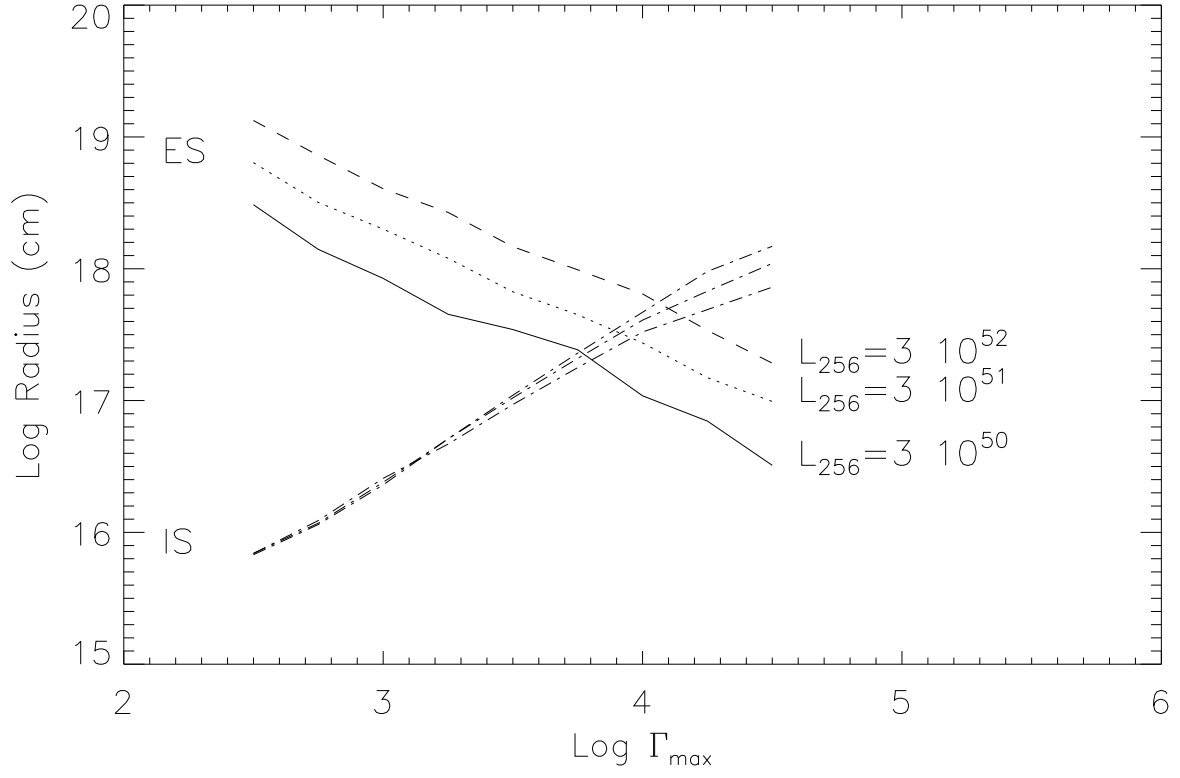


Figure 5

